Supporting Information

Identification of Small-Molecule Inhibitors of Fibroblast Growth Factor 23 Signaling via *In Silico* Hot Spot Prediction and Molecular Docking to α-Klotho

Shih-Hsien Liu[1,2,#], Zhousheng Xiao[3,#], Sambit K. Mishra[4], Julie C. Mitchell[4], Jeremy C. Smith[1,2], L. Darryl Quarles[3], Loukas Petridis[1,2*]

[1] UT/ORNL Center for Molecular Biophysics, Oak Ridge National Laboratory, Oak Ridge, Tennessee 37831, United States

[2] Department of Biochemistry and Cellular and Molecular Biology, University of Tennessee, Knoxville, Tennessee 37996, United States

[3] Department of Medicine, College of Medicine, University of Tennessee Health Science Center, Memphis, Tennessee 38163, United States

[4] Biosciences Division, Oak Ridge National Laboratory, Oak Ridge, Tennessee 37831, United States

[#]Equal contribution

*Corresponding author:

Email: petridisl@ornl.gov

Phone: +1-865-576-2576

S1. MD Simulations of α-Klotho

We used the steepest descent algorithm for energy minimization, which was considered converged when the maximum force < 1000 kJ/mol/nm. We used the v-rescale thermostat[1] with 0.2 ps as the time constant for coupling with two temperature coupling groups each for α-Klotho and water. We used the Berendsen[2] and Parrinello-Rahman[3] barostats with 2 ps as the time constant for coupling for equilibration and production, respectively. The isothermal compressibility for pressure coupling was 0.000044 bar^{-1}.[4] We used Verlet cutoff-scheme, fast smooth particle mesh Ewald (PME)[5] electrostatics, and linear constraint solver (LINCS)[6] algorithm on hydrogen-containing bonds.

To find the time period in production where structures of α-Klotho were equilibrated for clustering, three properties of α-Klotho were examined as a function of simulation time: 1) root-mean-square deviation (RMSD) of backbone atoms with respect to the crystal structure[7] (Figure S1), 2) radius of gyration, R_g (Figure S2), and 3) non-bonded potential energies (E_{pot}) of all atoms (Figure S3). Figures S1-S3 show that structures of α-Klotho in the last 100 ns for each of the five instances are well equilibrated.

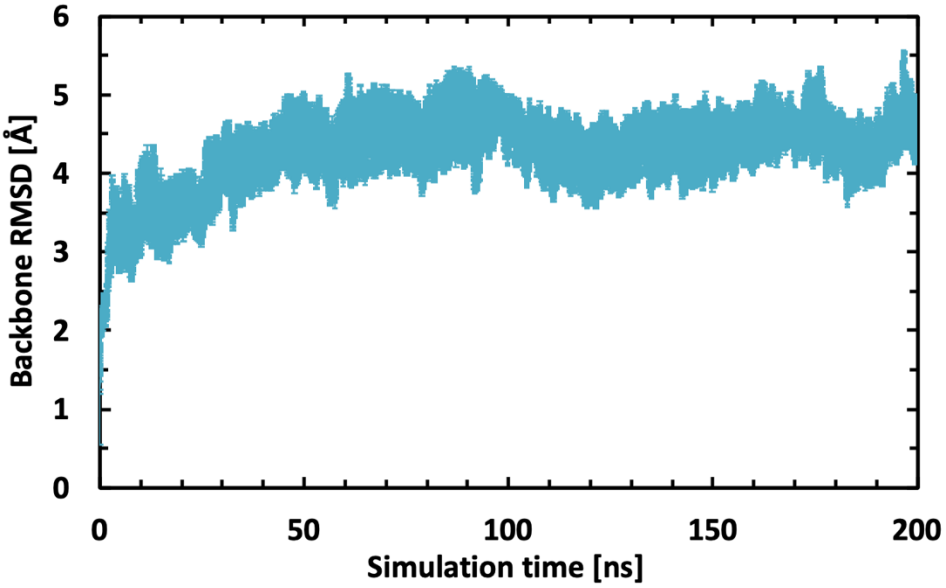

Figure S1. RMSD of backbone atoms on α-Klotho from crystal structure[7] *vs.* simulation time with error bars among the five instances. The average over the last 100 ns is 4.41 ± 0.00 Å.

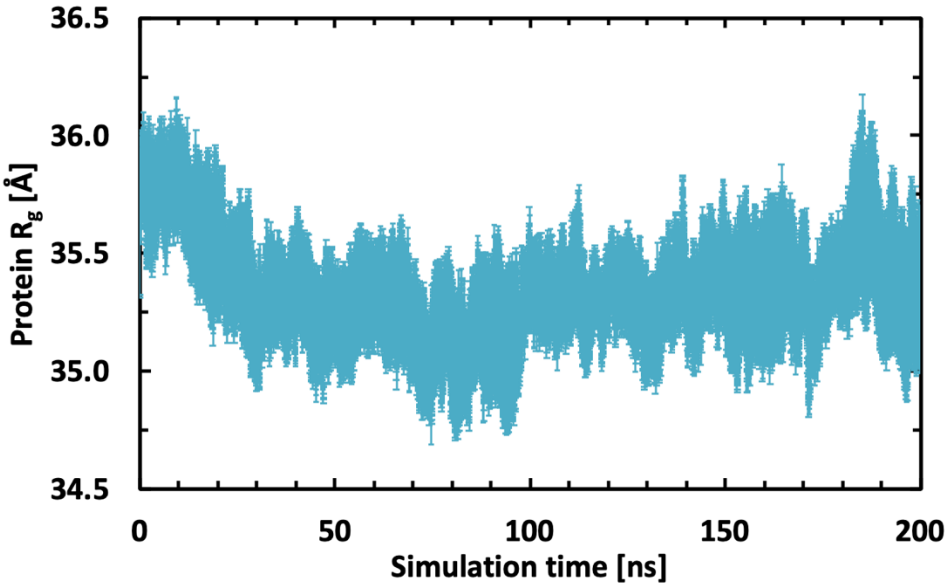

Figure S2. R_g of amino acid residues on α-Klotho *vs.* simulation time with error bars among the five instances. The average over the last 100 ns is 35.36 ± 0.00 Å.

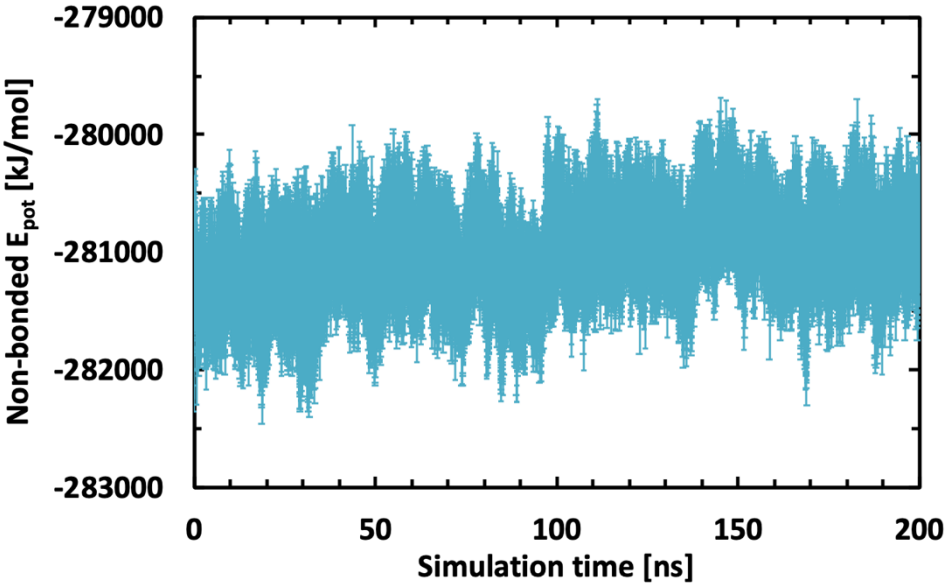

Figure S3. Non-bonded E_{pot} of all atoms on α-Klotho *vs.* simulation time with error bars among the five instances. The average over the last 100 ns is -280874 ± 2 kJ/mol.

S2. Clustering of α-Klotho

Table S1. Test of RMSD cutoff on interface residues. For each tested cutoff, the number of total and 1-frame clusters and the percentage of MD frames for clusters #1-10 are shown. The RMSD cutoff chosen and its results are shown in red.

RMSD cutoff [Å]		**1.50**	**1.51**	**1.52**	**1.53**	**1.54**	**1.55**	**1.6**	**1.7**	**1.8**	**1.9**	**2.0**
# total clusters		44	41	38	37	35	34	29	16	11	7	6
# 1-frame clusters		3	3	1	2	2	3	2	2	1	1	2
frame % for cluster #	**1**	75.7	77.1	78.4	79.7	81.2	82.6	88.1	94.8	97.9	99.2	99.7
	2	7.7	7.5	7.2	8.0	7.5	6.9	5.0	2.2	1.1	0.5	0.2
	3	3.9	3.7	3.5	3.4	3.3	3.1	2.2	1.2	0.5	0.1	0.0
	4	3.8	3.5	2.3	2.0	1.8	1.7	1.2	0.7	0.2	0.1	0.0
	5	2.1	2.1	2.0	1.6	1.6	1.5	1.1	0.4	0.2	0.0	0.0
	6	1.5	1.3	1.9	1.2	1.1	1.1	0.8	0.2	0.1	0.0	0.0
	7	1.2	1.1	1.5	1.0	0.9	0.8	0.5	0.2	0.0	0.0	
	8	0.8	0.7	0.6	0.9	0.8	0.7	0.3	0.1	0.0		
	9	0.7	0.7	0.5	0.4	0.4	0.3	0.2	0.1	0.0		
	10	0.6	0.5	0.5	0.4	0.4	0.3	0.1	0.0	0.0		
	sum	98.1	98.3	98.4	98.7	98.9	99.0	99.5	99.9	100.0	100.0	100.0

S3. Coordination of the Zn Atom on All α-Klotho Structures in the Ensemble Docking

Table S2. The distances in Å between the Zn atoms and Cα atoms of Asp426, Cys739, Asp745, and Asp815 (the 4 residues with which the Zn atom coordinates in the crystal structure) for the crystal structure[7] and 10 MD clusters of α-Klotho.

receptor / residue	crystal	cluster #									
		1	**2**	**3**	**4**	**5**	**6**	**7**	**8**	**9**	**10**
Asp426	5.0	5.6	5.4	5.6	5.5	5.6	4.7	5.0	4.9	5.6	5.6
Cys739	4.2	5.3	5.0	5.2	5.4	5.0	5.0	5.6	5.0	5.2	5.2
Asp745	5.4	5.4	5.3	5.5	5.0	4.9	4.9	4.8	4.9	5.5	5.2
Asp815	4.5	4.6	4.5	4.5	4.5	4.4	4.2	4.7	4.6	4.6	4.6

S4. Docking to α-Klotho

Table S3. The Cartesian coordinates of centers of ligand pose-searching boxes for the crystal structure[7] and 10 MD clusters of α-Klotho.

box center / receptor		x	y	z
	crystal	146.44	132.49	57.13
cluster #	**1**	146.21	133.13	56.83
	2	145.99	132.92	56.68
	3	145.69	133.78	56.47
	4	146.37	132.79	56.91
	5	146.68	132.97	56.47
	6	146.67	132.44	56.96
	7	146.56	132.94	56.56
	8	146.87	132.84	56.74
	9	146.95	133.22	56.41
	10	145.63	134.20	56.36

Table S4. The distances in Å between centers of ligand pose-searching boxes and Cα atoms of interface residues for the crystal structure[7] and 10 MD clusters of α-Klotho. Values in red indicate that Cα atoms are located outside of boxes. We note that Ser471 and Gln844 are not computationally predicted hot spots at the KL1:KL2:FGF23 interface of α-Klotho (See Table 1 in the main text).

receptor / residue	crystal	cluster #									
		1	**2**	**3**	**4**	**5**	**6**	**7**	**8**	**9**	**10**
Lys429	5.9	5.0	5.4	5.1	5.4	5.3	5.2	5.4	5.5	5.0	5.0
Tyr433	6.1	6.2	6.1	6.1	6.1	6.2	6.1	6.1	6.0	6.1	6.0
Phe437	10.5	10.9	11.2	11.0	11.0	10.8	11.1	10.9	10.7	11.1	11.3
Ser471	21.3	21.6	22.0	21.5	21.7	20.9	21.8	21.1	22.5	20.3	20.5
Lys823	16.4	15.8	15.8	16.3	18.1	17.2	15.7	16.5	16.0	17.4	16.7
Met833	8.3	9.2	9.1	8.5	8.8	9.7	8.6	9.4	9.2	10.7	8.8
Thr834	7.3	7.3	7.5	7.5	7.1	8.4	7.4	7.8	7.7	8.3	7.5
Ile836	7.2	6.5	6.5	7.0	6.7	8.0	6.8	7.0	6.9	8.2	6.4
Gln844	16.2	16.8	16.9	16.9	16.5	16.7	17.8	16.7	18.4	17.2	16.3

S5. Hot Spot Analysis on the FGF23:FGFR1c:α-Klotho Ternary Complex

Table S5. The 9 residues defining the D3:FGF23 interface in the ternary crystal structure,[7] and additional 2 residues in bold were predicted as druggable sites using FTMap.[8] The hot-spot identification and confidence scores were evaluated by the KFC2a method.[9] Positive confidence scores suggest prospective hot spots, and 4 out of 9 interface residues are predicted hot spots. N/A: not available.

Protein	Residue	Number	Hot spot	Confidence score
FGFR1c D3 domain	Arg	250	Yes	0.49
	Tyr	**280**	**No**	**-1.95**
	Ser	**281**	**N/A**	**N/A**
	Asp	282	No	-2.25
	Pro	283	Yes	0.19
FGF23 N-terminal domain	His	117	Yes	0.24
	Thr	119	No	-0.99
	Gly	123	No	-1.21
	Asp	125	Yes	0.11
	Tyr	127	N/A	N/A
	Ser	159	No	-0.58

Table S6. The 4 residues defining the KL2:FGF23 interface in the ternary crystal structure.[7] The hot-spot identification and confidence scores were evaluated by the KFC2a method.[9] Positive confidence scores suggest prospective hot spots, and 3 out of 4 interface residues are predicted hot spots.

Protein	Residue	Number	Hot spot	Confidence score
α-Klotho KL2 domain	Asp	756	No	-0.38
FGF23 C-terminal tail	Lys	194	Yes	0.71
	Arg	196	Yes	1.76
	Arg	198	Yes	1.48

Table S7. The 11 residues defining the D2:FGF23 interface in the ternary crystal structure.[7] The hot-spot identification and confidence scores were evaluated by the KFC2a method.[9] Positive confidence scores suggest prospective hot spots, and 7 out of 11 interface residues are predicted hot spots.

Protein	Residue	Number	Hot spot	Confidence score
FGFR1c D2 domain	Glu	162	No	-1.39
	Leu	165	Yes	1.23
	Ala	167	Yes	1.32
	Gln	244	No	-1.10
	Val	248	Yes	0.94
FGF23 N-terminal domain	Tyr	43	Yes	1.19
	Asn	49	Yes	0.03
	Ser	50	Yes	0.06
	His	66	No	-0.74
	Tyr	124	No	-0.29
	Leu	158	Yes	1.34

Table S8. The 20 residues defining the RBA:D3 interface in the ternary crystal structure.[7] The hot-spot identification and confidence scores were evaluated by the KFC2a method.[9] Positive confidence scores suggest prospective hot spots, and 10 out of 20 interface residues are predicted hot spots. N/A: not available.

Protein	Residue	Number	Hot spot	Confidence score
α-Klotho RBA	Val	546	Yes	0.54
	Tyr	547	Yes	0.42
	Leu	548	Yes	1.19
	Trp	549	Yes	1.66
	Lys	555	Yes	0.33
	Arg	556	No	-2.71
	Leu	557	Yes	1.01
	Ile	558	No	-1.81
	Val	560	No	-1.81
	Val	563	N/A	N/A
	Val	564	No	-1.68
FGFR1c D3 domain	Leu	290	Yes	1.37
	Ile	293	No	-0.07
	Val	295	No	-0.69
	Leu	305	Yes	0.41
	Tyr	307	No	-0.91
	Val	308	Yes	1.04
	Ile	310	Yes	0.81
	Leu	342	No	-0.56
	Leu	349	No	-1.89

S6. Surface Pocket Analysis on α-Klotho in the Ternary Complex

Table S9. The residues participating in the surface pockets (See Figure 2 in the main text) in α-Klotho crystal structure[7] using CASTp.[10]

Pocket 1		Pocket 2	
Residue	**Number**	**Residue**	**Number**
Trp	42	Pro	51
Arg	44	Glu	52
Phe	45	Gly	55
Ser	46	Leu	56
Arg	47	Phe	57
Pro	48	Arg	425
Pro	49	Met	431
Ala	50	Tyr	432
Pro	51	Lys	435
Ala	53	Met	439
Ala	54	Pro	490
Asn	304	Lys	491
Pro	305	Ser	492
Arg	306	Leu	495
Met	308	Phe	496
Leu	389	Lys	499
Glu	390	Leu	500
Ser	391	Lys	503
Pro	392	Gly	505
Asn	393	Phe	506
Leu	394	Pro	507
Arg	395	Leu	509
Gln	396	Glu	511
Lys	429	Asn	512
Tyr	432	Gln	513
Tyr	433	Pro	514
Lys	436	Glu	736
Phe	437	Pro	737
Glu	440	Ala	738
Lys	443	Cys	739
Leu	447	Pro	740
Asp	448	Phe	741
Glu	819	Ser	742
Asp	820	Leu	813
Lys	823	Asp	835

Gln	831	Thr	837
Glu	832	Trp	838
Met	833	Leu	839
Thr	834	Val	847
Asp	835	Val	848
Ile	836	Pro	849
Thr	837	Trp	850
Trp	838	Arg	853
Leu	839	Lys	854
Asn	840	Tyr	889
Ser	841	Gln	892
Pro	842	Asn	893
Gln	844	Asn	896
Gly	878	Glu	897
Leu	879	Lys	900
Glu	882	Leu	904
Gln	885		
Leu	886		

S7. Contact Analysis on the 45 Compounds

Table S10. The average non-hydrogen atomic contacts ($\overline{\boldsymbol{Contact}}$) with stand errors of ligands listed in Tables 2 and 3 and shown in Figure 4 in the main text with residues in surface pockets in α-Klotho structures. The numbers of contacts are rounded to the nearest integer, and only residues with $\overline{\boldsymbol{Contact}}$ > 1 are listed.

Ligands in Table 2 (orange ones in Figure 4)						**Ligands in Table 3 (red ones in Figure 4)**	
crystal		**cluster #8**		**cluster #2**		**crystal**	
Residue Number	$\overline{\boldsymbol{Contact}}$	**Residue Number**	$\overline{\boldsymbol{Contact}}$	**Residue Number**	**Contact**	**Residue Number**	$\overline{\boldsymbol{Contact}}$
Trp850	17 ± 2	Leu56	25 ± 1	Phe57	17	Tyr433	23 ± 0
Phe57	14 ± 1	Trp850	8 ± 0	Trp838	9	Lys436	10 ± 1
Trp838	11 ± 1	Leu839	8 ± 2	Lys435	8	Ile836	9 ± 0
Asn512	6 ± 1	Gly55	7 ± 1	Phe506	6	Pro392	7 ± 0
Lys435	4 ± 0	Asn512	6 ± 0	Trp850	5	Lys429	6 ± 1
Pro849	2 ± 0	Trp838	5 ± 1	Leu839	4	Phe437	4 ± 0
Thr837	2 ± 0	Glu52	3 ± 2	Thr837	4	Asn393	3 ± 1
Phe506	2 ± 1	Phe57	3 ± 0	Leu56	3	Tyr432	2 ± 0
Asp835	2 ± 1	Pro849	2 ± 0	Tyr889	3	Met833	2 ± 0
		Thr837	2 ± 1	Val847	3		
		Ala53	2 ± 1				

S8. Surface Pocket Analysis on α-Klotho MD Clusters

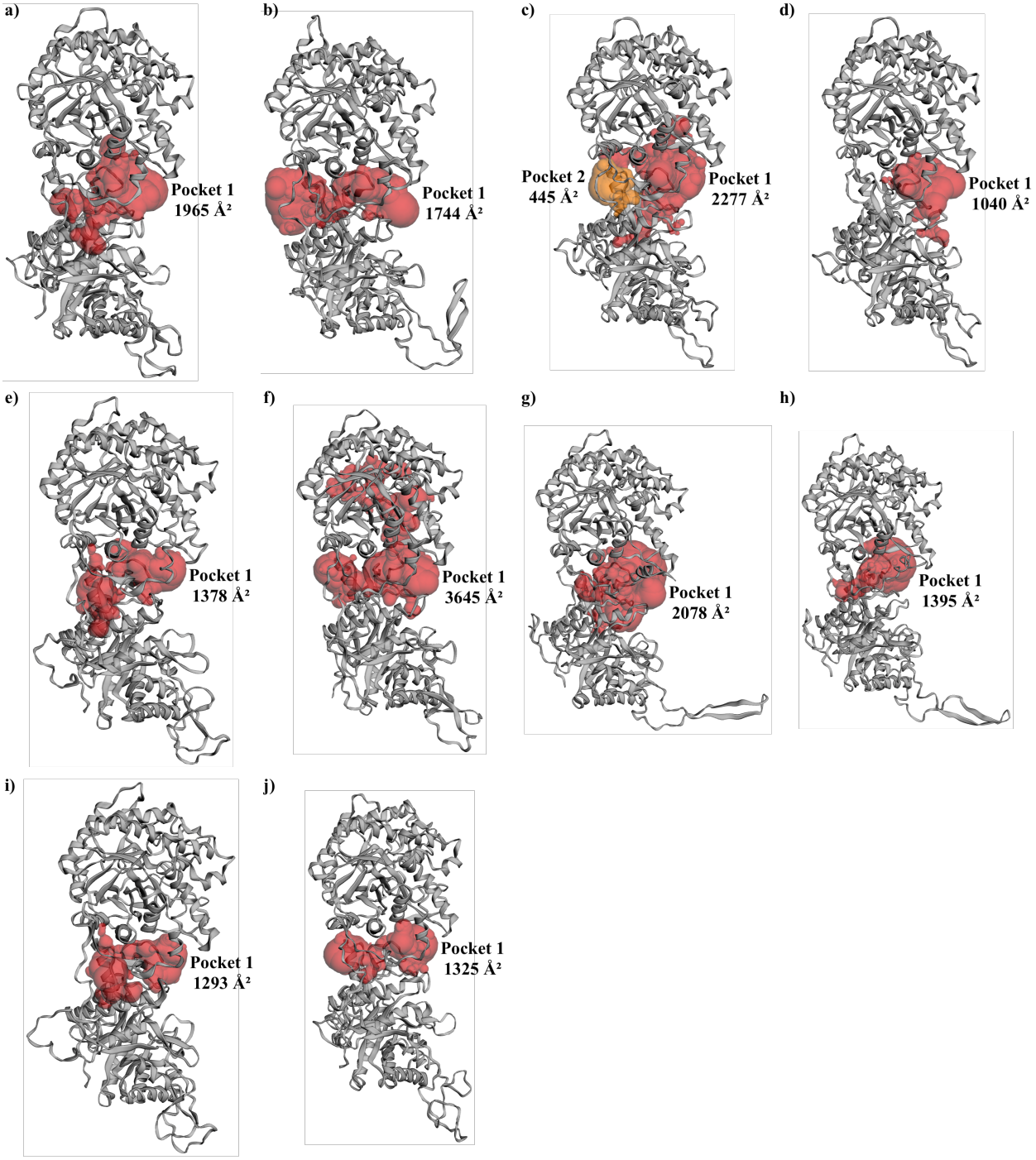

Figure S4. The surface Pockets 1 (red) and 2 (orange), which derive from Figure 2 in the main text, with their SASA in Å^2 calculated using CASTp[10] for α-Klotho MD clusters #1-10 (a-j). The residues participating in these pockets are listed in Table S11.

Table S11. The residues participating in surface Pockets 1 and 2 (See Figure S4) in α-Klotho MD clusters #1-10 using CASTp.[10]

#1	#2	#3	#4	#5	#6	#7	#8	#9	#10
Asp37	Thr41	**Pocket 1**	Gln40	Trp42	Gln40	Thr41	Phe45	Thr41	Thr41
Gly38	Arg44	Thr41	Thr41	Phe45	Thr41	Ala43	Ser46	Trp42	Arg44
Gln40	Phe45	Trp42	Arg44	Ser46	Arg44	Arg44	Arg47	Phe45	Phe45
Thr41	Ser46	Arg44	Phe45	Pro48	Phe45	Phe45	Pro48	Ser46	Arg47
Arg44	Arg47	Phe45	Ser46	Pro49	Ser46	Ser46	Pro49	Arg47	Pro48
Phe45	Pro48	Ser46	Arg47	Ala50	Arg47	Arg47	Ala50	Pro48	Pro49
Ser46	Pro49	Arg47	Pro48	Pro51	Pro48	Pro48	Pro51	Pro49	Ala50
Arg47	Ala50	Pro48	Pro49	Glu52	Pro49	Pro49	Glu52	Pro51	Pro51
Pro48	Pro51	Pro49	Ala50	Glu52	Ala50	Ala50	Ala53	Glu52	Glu52
Pro49	Glu52	Ala50	Ala53	Ala53	Pro51	Pro51	Ala54	Ala53	Ala53
Ala50	Ala53	Pro51	Ala54	Ala54	Glu52	Glu52	Gly55	Ala54	Ala54
Pro51	Ala54	Ala53	Gly55	Gly55	Ala53	Ala53	Leu56	Gly55	Gly55
Glu52	Gly55	Ala54	Leu56	Leu56	Ala54	Gly55	Phe57	Leu56	Leu56
Ala53	Leu56	Gly55	Phe57	Phe57	Gly55	Leu56	Gln58	Phe57	Phe57
Ala54	Phe57	Ser300	Asn304	Gln58	Leu56	Phe57	Asn304	Gln58	Gln58
Gly55	Gln58	Trp302	Pro305	Phe61	Phe57	Gln58	Phe371	Phe61	Asn304
Leu56	Asn304	Ile303	Arg306	Trp67	Gln58	Asn304	Gly372	Trp67	Pro305
Phe57	Pro305	Asn304	Arg307	Trp302	Ser71	Pro305	Pro373	Trp302	Met308
Gln58	Arg306	Pro305	Met308	Asn304	Ala72	Arg306	Phe377	Asn304	Leu389
Asn304	Arg307	Arg306	Leu389	Pro305	Ala73	Arg307	Gln378	Pro305	Glu390
Pro305	Met308	Met308	Glu390	Arg306	Tyr74	Phe377	Leu389	Met308	Ser391
Arg306	Leu389	Ile313	Ser391	Met308	Gln75	Gln378	Glu390	Leu389	Pro392
Arg307	Ser391	Ser319	Pro392	Leu389	Thr76	Lys385	Ser391	Glu390	Asn393
Met308	Pro392	Leu320	Asn393	Glu390	Glu77	Arg387	Pro392	Ser391	Arg395
Pro373	Asn393	Val323	Arg395	Ser391	Gly78	Gln388	Asn393	Pro392	Gln396
Ser376	Arg395	Phe371	Gln396	Pro392	Gly79	Leu389	Arg395	Asn393	Ser399
Phe377	Gln396	Gly372	Ser399	Asn393	Trp80	Glu390	Gln396	Arg395	Met431
Leu389	Ser399	Pro373	Leu403	Arg395	Gln82	Ser391	Trp417	Gln396	Tyr432
Glu390	Met431	Leu375	Lys436	Gln396	Lys85	Pro392	Phe418	Lys429	Lys435
Ser391	Tyr432	Ser376	Met439	Val419	Gly86	Asn393	Val419	Met431	Lys436
Pro392	Tyr433	Phe377	Glu440	Ser420	Asp91	Arg395	Ser420	Tyr432	Met439
Asn393	Lys435	Leu380	Lys443	Thr422	Thr92	Gln396	Thr422	Tyr433	Glu440
Arg395	Lys436	Lys385	Leu447	Thr423	Phe93	Trp417	Thr423	Lys435	Lys443
Gln396	Met439	Gln388	Asp448	Lys424	Thr94	Phe418	Asp426	Lys436	Leu447
Ser399	Glu440	Leu389	Asp835	Asp426	Pro97	Val419	Asp427	Ile438	Asp448
Trp400	Lys443	Glu390	Ile836	Asp427	Gln118	Ser420	Ala428	Met439	Leu495
Leu403	Asp448	Ser391	Thr837	Ala428	Pro119	Thr423	Lys429	Glu440	Phe496
Trp417	Leu495	Pro392	Trp838	Lys429	Ala120	Asp426	Tyr430	Lys443	Lys499
Phe418	Phe496	Asn393	Leu839	Tyr432	Thr121	Asp427	Tyr432	Phe496	Leu500
Val419	Lys499	Arg395	Asn840	Tyr433	Ala125	Ala428	Tyr433	Leu500	Lys503

Ser420	Leu500	Gln396	Ser841	Lys435	Ser126	Lys429	Lys436	Gly505	Gly505
Lys429	Glu502	Ser399	Pro842	Lys436	Asp127	Tyr432	Phe437	Phe506	Phe506
Tyr432	Lys503	Asn415	Gln844	Ile438	Ser128	Tyr433	Met439	Pro508	Pro507
Tyr433	Gly505	Gly416	Val847	Met439	Tyr129	Lys435	Glu440	Leu509	Glu511
Lys436	Phe506	Trp417	Ile875	Glu440	Asn131	Lys436	Lys443	Asn512	Asn512
Met439	Pro507	Val419	Asp876	Lys443	Val132	Met439	Leu447	Gln513	Glu736
Glu440	Pro508	Ser420	Asp877	Phe496	Arg134	Glu440	Pro507	Pro514	Pro737
Lys443	Leu509	Thr422	Gly878	Leu500	Asp135	Lys443	Leu509	Glu736	Ala738
Leu447	Pro510	Thr423	Leu879	Gly505	Thr136	Leu447	Pro510	Pro737	Pro740
Asp448	Glu511	Lys424	Ala881	Phe506	Leu139	Phe506	Glu511	Pro740	Phe741
Arg468	Asn512	Arg425	Glu882	Leu509	Tyr147	Pro510	Asn512	Leu813	Leu813
Ile472	Gln513	Asp426	Asp883	Glu511	Arg148	Glu511	Gln513	Met833	Asp835
Glu511	Pro514	Asp427	Asp884	Asn512	Phe149	Asn512	Ile812	Thr834	Ile836
Asn512	Glu736	Ala428	Gln885	Gln513	Ser150	Pro690	Glu817	Asp835	Thr837
Gln513	Pro737	Lys429	Leu886	Pro514	Ile151	Tyr691	Glu819	Ile836	Trp838
Pro514	Pro740	Tyr432	Arg887	Leu515	Ser152	Thr692	Asp820	Thr837	Leu839
Thr810	Phe741	Tyr433	Asp919	Glu516	Trp153	Arg693	Ile822	Trp838	Asn840
Thr811	Leu813	Lys436	Arg924	Ala738	Arg155	Asn694	Lys823	Leu839	Pro842
Ile812	Thr834	Phe437	Arg929	Leu813	Tyr172	Leu730	Gln831	Asn840	Gln844
Glu819	Asp835	Met439	Tyr930	Asp815	Tyr173	Gln731	Glu832	Ser841	Val847
Asp820	Ile836	Lys443	Ala931	Glu817	Leu176	Asp733	Met833	Pro842	Val848
Pro821	Thr837	Leu447	Lys938	Lys818	Thr190	Trp734	Thr834	Gln844	Pro849
Ile822	Trp838	Asp448	Ser940	Glu819	Leu191	Ile735	Asp835	Val847	Trp850
Lys823	Leu839	Tyr478		Met833	Tyr192	Val752	Ile836	Val848	Lys854
Gln831	Asn840	Ser492		Thr834	Trp194	Leu753	Thr837	Pro849	Gly878
Glu832	Ser841	Leu495		Asp835	Asp195	Asp756	Trp838	Trp850	Leu879
Met833	Pro842	Pro690		Ile836	Leu196	Ile757	Leu839	Gly878	Asp883
Thr834	Gln844	Tyr691		Thr837	Pro197	Leu760	Asn840	Leu879	Asp884
Asp835	Val847	Thr692		Trp838	Tyr219	Ser807	Gln844	Ala881	Gln885
Ile836	Val848	Arg693		Leu839	Asp238	Tyr809	Ala846	Glu882	Leu886
Thr837	Pro849	Met695		Asn840	Asn239	Thr810	Val847	Asp883	Tyr889
Trp838	Trp850	Leu730		Ser841	Tyr241	Thr811	Val848	Gln885	Asn893
Leu839	Arg853	Gln731		Gln844	Val242	Ile812	Pro849	Leu886	Asn896
Asn840	Lys854	Ala732		Val847	Trp245	Leu813	Trp850	Val888	Glu897
Ser841	Asn857	Asp733		Val848	Gly247	Val814	Tyr889	Tyr889	
Pro842	Gly878	Ile735		Pro849	Thr250	Asp815	Asn893	Gln892	
Gln844	Leu879	Ala738		Trp850	Arg252	Glu817	Glu897	Asn893	
Val845	Ala881	Phe741		Arg853	Leu253	Glu819		Asn896	
Ala846	Leu886	Ser742		Lys854	Ser299	Asp820		Glu897	
Val847	Tyr889	Gln743		Leu879	Ser300	Pro821		Lys900	
Val848	Asn893	Lys744		Ala881	Trp302	Ile822		Phe953	
Pro849	Asn896	Asp745		Glu882	Ile303	Lys823			
Trp850	Glu897	Val752		Gln885	Asn304	Asn825			
Ile875	Lys900	Asp756		Leu886	Pro305	Leu828			

Gly878	Leu904	Ile757	Tyr889	Arg306	Val830
Leu879	Asp905	Trp759	Gln892	Arg307	Gln831
Asp884		Leu760	Asn893	Met308	Glu832
Gln885		Ala761	Asn896	Ser319	Met833
Leu886		Phe765	Glu897	Leu320	Thr834
Val888		Leu804	Lys900	Val323	Asp835
Tyr889		Leu806	Phe953	Leu324	Ile836
Tyr890		Thr810		Cys370	Thr837
Met891		Thr811		Phe371	Trp838
Gln892		Ile812		Gly372	Leu839
Asn893		Leu813		Pro373	Asn840
Tyr894		Val814		Thr374	Ser841
Asn896		Asp815		Leu375	Pro842
Glu897		Ser816		Ser376	Ser843
Lys900		Glu817		Phe377	Gln844
Ala939		Lys818		Gln378	Val845
Ser940		Glu819		Leu379	Ala846
Lys942		Asp820		Leu380	Val847
Tyr944		Lys823		Asp381	Val848
Lys946		Tyr824		Lys385	Pro849
Ile947		Asn825		Leu389	Trp850
Phe953		Leu828		Glu390	Ile875
		Val830		Ser391	Asp876
		Gln831		Pro392	Asp877
		Glu832		Asn393	Gly878
		Met833		Arg395	Leu879
		Thr834		Gln396	Ala881
		Asp835		Leu397	Glu882
		Ile836		Ser399	Asp883
		Thr837		Leu403	Gln885
		Trp838		Glu414	Leu886
		Leu839		Gly416	Arg887
		Asn840		Trp417	Tyr889
		Ser841		Phe418	
		Pro842		Val419	
		Gln844		Ser420	
		Val845		Lys429	
		Ala846		Met431	
		Leu859		Tyr432	
		Ile875		Tyr433	
		Asp876		Lys435	
		Asp877		Lys436	
		Gly878		Phe437	
		Leu879		Met439	

Ala881
Glu882
Asp883
Asp884
Leu886
Arg887
Arg929

Pocket 2

Phe57
Gln58
Met431
Tyr432
Lys435
Met439
Phe496
Lys499
Leu500
Lys503
Gly505
Phe506
Pro507
Leu509
Glu511
Asn512
Glu736
Pro737
Ala738
Pro740
Phe741
Leu813
Asp835
Trp838
Leu839
Val847
Val848
Pro849
Trp850
Lys854
Tyr889
Asn893
Asn896
Glu897

Glu440
Lys443
Leu447
Asp448
Trp458
Ser459
Leu460
Met461
Asp462
Gly463
Phe464
Glu465
Trp466
Arg468
Tyr470
Ser471
Ile472
Arg473
Arg474
Val479
Asp480
Phe481
Leu488
Phe496
Lys499
Leu500
Lys503
Gly505
Phe506
Pro507
Leu509
Glu511
Asn512
Gln513
Pro514
Glu736
Pro737
Pro740
Phe741
Thr810
Thr811
Ile812
Leu813
Glu819

Asp820
Lys823
Gln831
Glu832
Met833
Thr834
Asp835
Ile836
Thr837
Trp838
Leu839
Asn840
Ser841
Pro842
Gln844
Val845
Ala846
Val847
Val848
Pro849
Trp850
Arg853
Lys854
Asp876
Asp877
Gly878
Leu879
Ala881
Asp884
Gln885
Leu886
Arg887
Tyr889
Asn893
Glu897

S9. Correlation Between ΔG (Vina) and ΔG (K_{DEEP})

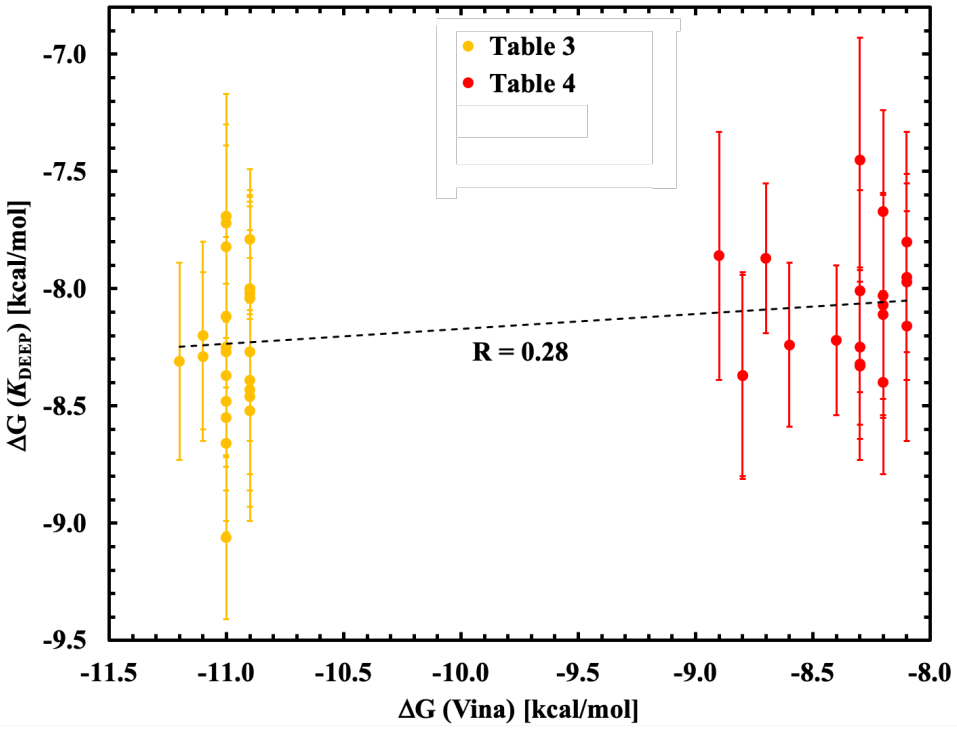

Figure S5. The linear dashed trendline between ΔG (Vina) and ΔG (K_{DEEP}) in Tables 2 and 3 in the main text with Pearson's correlation coefficient (R).[11] The capped bars show standard deviation of ΔG (K_{DEEP}).

S10. Top 50 Compounds Ranked by $\overline{\Delta G\ (Vina)}$ Over All α-Klotho Structures in the Ensemble Docking

Table S12. The 50 compounds ranked by the lowest average estimated free energies of binding ($\overline{\Delta G\ (Vina)}$) over all α-Klotho structures in the ensemble docking. The compound selected for *in vitro* assays is in bold. The compounds in green also appear in Table 2 in the main text. The underscored compounds with the same ZINC ID have different protonation states in the database.[12]

ZINC ID	$\overline{\Delta G\ (Vina)}$ [kcal/mol]	ZINC ID	$\overline{\Delta G\ (Vina)}$ [kcal/mol]
12409120	**-9.95**	65236018	-9.51
03617904	-9.78	75536601	-9.51
79095260	-9.69	65248351	-9.50
98150430	-9.68	00620607	-9.50
98150430	-9.67	12515638	-9.50
33020023	-9.65	98150430	-9.50
45202181	-9.65	76357267	-9.49
17322022	-9.64	74377515	-9.49
77974929	-9.64	75536652	-9.49
08976410	-9.58	05052491	-9.48
72164992	-9.57	44329833	-9.48
52491820	-9.56	45202184	-9.48
96132781	-9.56	84594986	-9.48
98150430	-9.56	64890579	-9.47
79095266	-9.55	69775761	-9.47
03908210	-9.55	58230019	-9.47
33020020	-9.55	98150430	-9.47
08997061	-9.54	12559984	-9.46
65248632	-9.54	40375888	-9.46
88338906	-9.54	45799368	-9.46
75536619	-9.53	88339043	-9.46
98150430	-9.52	36652493	-9.45
40375888	-9.51	75536661	-9.45
98150430	-9.51	72170062	-9.45
05313250	-9.51	98150430	-9.45

S11. *In Silico* ZINC05326903:α-Klotho Interaction Analysis

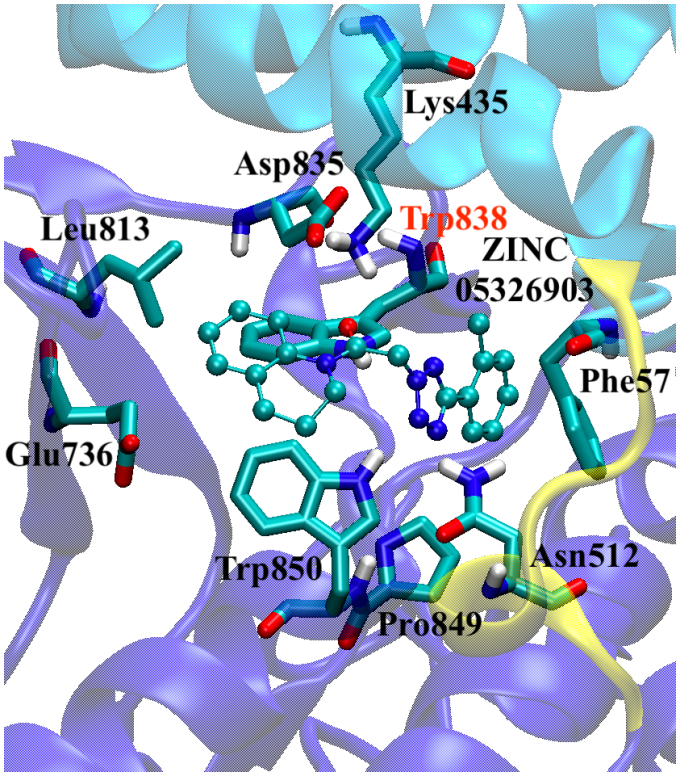

Figure S6. The binding pose of ZINC05326903 in the KL1-linker-KL2 (light blue-yellow-dark blue) region of α-Klotho crystal structure[7] in the ensemble docking. Only residues whose protein-ligand non-hydrogen atomic contacts > 1 are shown. The residue in red forms hydrogen bonds with the ligand.

References

(1) Bussi, G.; Donadio, D.; Parrinello, M. Canonical Sampling Through Velocity Rescaling. *J. Chem. Phys.* **2007**, *126*, 014101.

(2) Berendsen, H. J. C.; Postma, J. P. M.; van Gunsteren, W. F.; DiNola, A.; Haak, J. R. Molecular Dynamics with Coupling to an External Bath. *J. Chem. Phys.* **1984**, *81*, 3684-3690.

(3) Parrinello, M.; Rahman, A. Polymorphic Transitions in Single Crystals: A New Molecular Dynamics Method. *J. Appl. Phys.* **1981**, *52*, 7182-7190.

(4) Fine, R. A.; Millero, F. J. Compressibility of Water as a Function of Temperature and Pressure. *J. Chem. Phys.* **1973**, *59*, 5529-5536.

(5) Abraham, M. J.; Gready, J. E. Optimization of Parameters for Molecular Dynamics Simulation Using Smooth Particle-Mesh Ewald in GROMACS 4.5. *J. Comput. Chem.* **2011**, *32*, 2031-2040.

(6) Hess, B. P-LINCS: A Parallel Linear Constraint Solver for Molecular Simulation. *J. Chem. Theory Comput.* **2008**, *4*, 116-122.

(7) Chen, G.; Liu, Y.; Goetz, R.; Fu, L.; Jayaraman, S.; Hu, M.-C.; Moe, O. W.; Liang, G.; Li, X.; Mohammadi, M. α-Klotho is a Non-Enzymatic Molecular Scaffold for FGF23 Hormone Signaling. *Nature* **2018**, *553*, 461-466.

(8) Kozakov, D.; Grove, L. E.; Hall, D. R.; Bohnuud, T.; Mottarella, S. E.; Luo, L.; Xia, B.; Beglov, D.; Vajda, S. The FTMap Family of Web Servers for Determining and Characterizing Ligand-Binding Hot Spots of Proteins. *Nat. Protoc.* **2015**, *10*, 733-755.

(9) Zhu, X.; Mitchell, J. C. KFC2: A Knowledge-Based Hot Spot Prediction Method Based on Interface Solvation, Atomic Density, and Plasticity Features. *Proteins* **2011**, *79*, 2671-2683.

(10) Tian, W.; Chen, C.; Lei, X.; Zhao, J.; Liang, J. CASTp 3.0: Computed Atlas of Surface Topography of Proteins. *Nucleic Acids Res.* **2018**, *46*, W363-W367.

(11) Jiménez, J.; Škalič, M.; Martínez-Rosell, G.; De Fabritiis, G. K_{DEEP}: Protein-Ligand Absolute Binding Affinity Prediction via 3D-Convolutional Neural Networks. *J. Chem. Inf. Model.* **2018**, *58*, 287-296.

(12) Irwin, J. J.; Sterling, T.; Mysinger, M. M.; Bolstad, E. S.; Coleman, R. G. ZINC: A Free Tool to Discover Chemistry for Biology. *J. Chem. Inf. Model.* **2012**, *52*, 1757-1768.